UiT
THE ARCTIC
UNIVERSITY
OF NORWAY

Faculty of Science and Technology
Department of Mathematic and Statistics

# Origins and impacts of spatial and temporal long-range dependence in the climate system

—

**Hege-Beate Fredriksen**

*A dissertation for the degree of Philosophiae Doctor – September 2017*

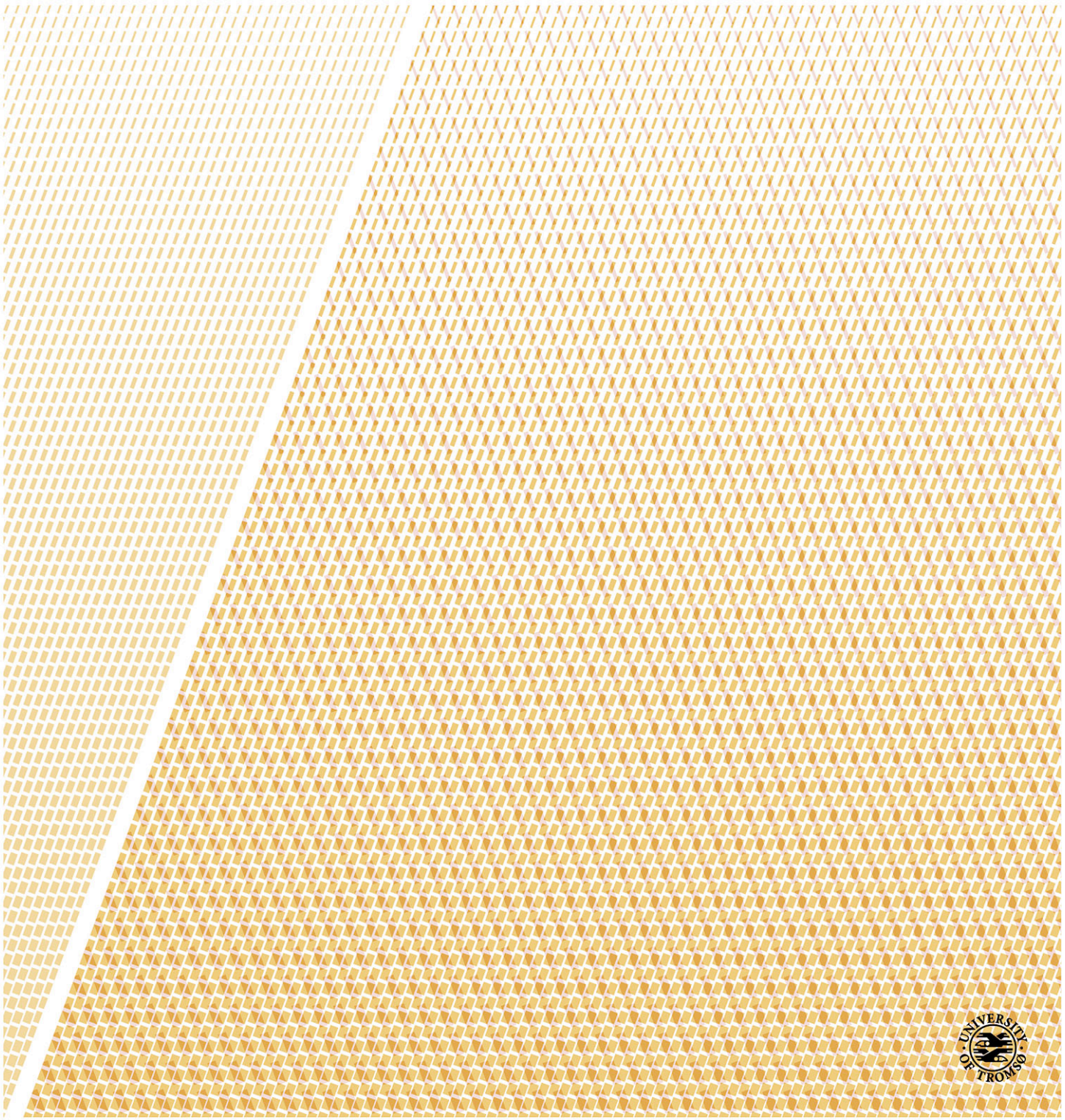

# Abstract

The internal variability of most Earth surface temperatures has a power spectral density well described by a power law, $S(f) \sim f^{-\beta}$, and we typically observe $0 < \beta < 1$. This characterizes variability exhibiting long-range dependence (LRD), which has no characteristic time scale. However, there is no consensus about the physical mechanisms behind this property, and the topic of this thesis is to explore where it comes from.

In Paper I, the spectral characteristics of detrended instrumental temperature records and temperatures simulated in climate models are studied. The persistence, as measured by $\beta$, is found to be stronger for sea than for land, and increasing with the degree of spatial averaging. An interpretation of the increase with spatial averaging is that high-frequency variability is averaged out to a larger degree than low-frequency variability. Paper II presents a spatiotemporal model with this property, and more specifically, it predicts that global $\beta$ is twice the value of the local $\beta$ on a uniform sphere. For temperatures in observation data and climate models, there are some regional differences in the spectral characteristics, but on average they are consistent with the model.

Paper III demonstrates how LRD in global temperature can be explained by a linear multibox energy balance model (EBM). In linear models, temperatures can be described as a response function convolved with the forcing. For the multibox EBM, the response function consists of a sum of exponential responses, which with the parameters estimated, is well approximated by a power-law response. Only three boxes, implying three response times, are needed to approximate the power-law response on scales from months to centuries. When driven by white noise forcing, a power-law response gives a process exhibiting LRD, which is well approximated by the sum of Ornstein-Uhlenbeck processes obtained for the exponential responses.

This thesis also puts these concepts into the context of simple climate models in general. The findings of multiple and long response times means that we can expect continued responses to past forcing for a long time into the future – longer than predicted from simple models that do not include interaction with the deep ocean.

# Acknowledgement

I would like to thank the Department of Mathematics and Statistics for giving me the opportunity to do a PhD, and my supervisors Martin and Kristoffer for all great inspiration, good ideas and deep understanding.

A special thanks to Kristoffer for suggesting a master project interesting and difficult enough that it provided enough inspiration and further questions for four more years of research, and for making your students feel included in the research group from the beginning. I appreciate being part of our nice little research group, with good company from present and previous members of our research group, Rebekka, Ola, Erik and Lene, and particularly for having Tine as my fellow PhD student and good friend for these years.

I am also grateful for the opportunity to go to conferences and workshops around the world, and several useful courses through the national research school ResClim.

Last but not least I would like to thank Marius, and my family and friends for all good support.

# Contents

# Chapter 1

# Introduction

When analyzing surface temperatures, for instance through their power spectral densities (PSDs), we observe that temperatures are varying on all time scales. The amplitude of the low-frequency variability relative to the high-frequency variability is stronger than expected for white noise, characteristic of a red-noise process. While the exact form of the red-noise spectra is somewhat loosely defined, it is commonly considered as the spectrum resulting from an Ornstein-Uhlenbeck (OU) stochastic process. Observed temperature spectra often differ from this, even if excluding externally forced changes, and are better described by a power law $S(f) \sim f^{-\beta}$ on scales from months to centuries. Since we observe no typical time scale of variability in such spectra, they are often called *scaling* or *scale invariant*. Sometimes they are also named $1/f$ noises or pink noises, because a typical exponent for many of the spectra is $\beta \approx 1$.

The spectral properties of a stochastic process are closely related to the temporal correlations. For a time series with a power-law spectrum the autocorrelation function (ACF) is also decaying as a power law. Hence positive temporal correlations are expected for all time lags, giving the process infinitely long memory. This property is called long-range dependence (LRD), or sometimes long-range memory (LRM). It has been observed in a wide range of geophysical records since H. E. Hurst first observed it in his studies of the river Nile (Hurst, 1951; Hurst et al., 1965). For this reason it is also often referred to as the Hurst effect, and the process is characterised by the *Hurst exponent*.

Even though this statistical property is shared by many different geophysical quantities, the physical mechanism behind it is not necessarily the same for all. Furthermore, the scaling property observed for one quantity over one range of time scales, e.g. weather scales, could have a different explanation from scaling observed on another range of time scales, e.g. decadal scales. In this thesis, the focus will be on the long-range dependence in surface temperatures on time scales from months to centuries. There is no consensus about the exact physical

mechanism behind this, but the lack of a characteristic time scale is commonly explained by the existence of numerous time scales, hence we cannot point out one that is characteristic. The atmospheric variability has one typical time scale, sea ice another, ocean circulation yet another, etc. But as we will get back to later, completely different hypotheses have also been proposed.

## 1.1 Scaling from response model

Rypdal and Rypdal (2014) hypothesised that the multitude of response times may be approximated mathematically as a scale-invariant power-law response, and demonstrated that such a response function can well describe the response to known external forcings, such as solar, volcanic and anthropogenic forcing. In addition, it can reproduce the long correlations and power-law spectra observed for the random temperature fluctuations by incorporating these into the model as the response to a white-noise stochastic forcing.

Underlying this hypothesis is also the hypothesis that the temperature response is linear. That is, the total temperature response may be split up into a linear combination of internal variability and the expected linear response to various external forcings. The assumption of linearity of the response is often used when analyzing output from complex climate models, despite our knowledge about nonlinear mechanisms in the climate system. However, as Box (1979) stated, *All models are wrong but some are useful*. In this context the linear power-law response is a useful approximation to the full response for small enough responses.

Simple response models, like this power-law response, are powerful tools to analyse past and future temperature projections. Contrary to the complex climate models that require several months of computation time on a supercomputer, a single response function can be used to compute global temperature projections in just a few seconds. Other response models have also been used previously, so what is new about the power-law response hypothesis is the mathematical form of the response.

The simplest linear response model we can derive from physical principles has a single exponential response. It can predict the expected temperature change in the historical period ($\sim$1850 - today) reasonably well, but fails to predict the decadal-millennial scale changes that become more apparent in long temperature simulations with idealized forcing scenarios. It also fails to well describe the residual temperature variability as a stochastic process generated by the same response function. The problems associated with this simple response can be solved by adding some more physical complexity, and hence more parameters to the model. Another way of resolving these problems is to simply replace the exponential response by a power-law response. This way we get a response model with better

abilities to describe the data that does not need additional parameters. However, there is no obvious physical mechanism leading to the power-law response, and the model fails to conserve energy due to the divergence when we let $t \to 0$ or $t \to \infty$.

## 1.2 Searching for the origin of LRD

Even though the power-law response model can explain the observed internal variability of the climate system, can we be sure that this is the best explanation of the LRD? And even if it is, we also need to investigate what the best physical explanation of the power-law response is. To begin our search for the origin of LRD, we started by analyzing the differences between LRD observed for local temperatures and LRD observed for global temperatures on time scales from months to centuries (Fredriksen and Rypdal, 2016). Maybe the spatial pattern could give some hints. The differences in the variability between land temperatures and sea surface temperatures indicated that the long correlations must arise in the ocean, which is also supported by our knowledge of the small heat capacity of air compared to water. The atmosphere is not capable of building up large enough reservoirs of heat to generate the multidecadal variability of the size observed in unforced climate variability.

What we also discovered, is that the most important contributions to the spectrum of global temperature is not the spectra of all local temperatures, but rather the sum of all cross-spectra between local temperatures. However, local temperatures with high spectral values also contribute with high cross-spectral values. After averaging, we end up with a spectral exponent $\beta$ that is higher for global temperature than it is on average for local temperatures. An explanation of this is that short-lasting fluctuations also have generally shorter spatial extent, while the longer-lasting fluctuations generally have a larger spatial extent. Hence the high-frequency variability will have more spatial degrees of freedom than the low-frequency variability, and be averaged out to a larger degree. The dependence of the spatial extent on the frequency leads to a frequency-dependent spatial correlation length – a feature that is captured by the spatio-temporal model by North et al. (2011). The temporal variations in this model are however characterised by an exponential response, and are hence not consistent with a LRD description.

After the success in Rypdal (2012) and Rypdal and Rypdal (2014) of replacing the exponential response in global temperature by a power-law response, we were inspired to try it in North's spatio-temporal model as well. We kept the same model for the spatial transport, but changed the temporal characteristics such that we obtained LRD in time. This turned out to also impact the form of the spatial correlations in the model. The results were published in Rypdal et al. (2015), and one of the major implications of this model is that it predicts that

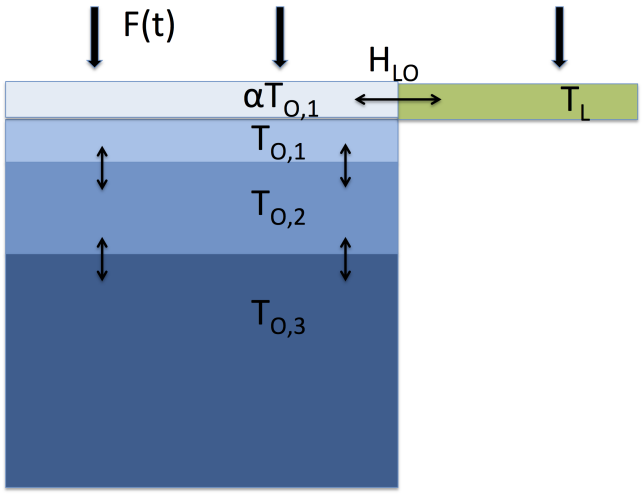


**Figure 1.1:** The three blue boxes show how we split up the ocean column in paper III. The green box is the atmosphere over land, that exchanges heat with the light gray box representing the atmosphere over ocean. $T_{O,1}$, $T_{O,2}$, $T_{O,3}$ and $T_L$ denote the temperature deviations from equilibrium in each of the boxes and $F(t)$ the surface forcing.

local temperatures have a spectral exponent equal to half the exponent for global temperature. This is close to what we observe on average.

With this paper, we found a way to model why global temperature is more persistent than local temperatures, but we were still lacking a simple way of modelling why sea surface temperatures (SST) are more persistent than land surface temperatures (LST). Although the idea that a long-range dependent process could be an approximation to a sum of multiple OU processes was known, we were also lacking a more specific explanation of how the multiple OU processes arise. So we decided to write a paper that demonstrates how we can get OU processes with several different time scales from simple box models (Fredriksen and Rypdal, 2017). We also demonstrated how the boxes could be constructed in order to explain the difference in the persistence between SST and LST (see Figure 1.1). By approximating the heat capacity of the land box by zero, the lower persistence of land is explained by a component instantly responding to the forcing.

## 1.3 Outline

Chapter 2 gives an overview of different simple climate models that are useful in order to understand where long-range dependence comes from. The assumption of

linearity is also discussed, necessary for describing LRD as something arising from a linear impulse response model. Chapter 3 reviews the literature studying LRD of surface temperatures, focusing more on explaining the qualitative properties, such as its origin and impacts, rather than quantitative studies of scaling exponents. Chapter 4 gives some concluding remarks, followed by the three published papers included in this thesis.

## 1.4 List of publications

**Paper I**
Fredriksen H.-B., and K. Rypdal (2016), **Spectral characteristics of instrumental and climate model surface temperatures**, *J. Climate*, 29, 1253–1268, doi:10.1175/JCLI-D-15-0457.1.

**Paper II**
Rypdal K., M. Rypdal, and H.-B. Fredriksen (2015), **Spatiotemporal Long-Range Persistence in Earth's Temperature Field: Analysis of Stochastic-Diffusive Energy Balance Models**, *J. Climate*, 28, 8379–8395, doi:10.1175/JCLI-D-15-0183.1.

**Paper III**
Fredriksen H.-B., and M. Rypdal (2017), **Long-range persistence in global surface temperatures explained by linear multibox energy balance models**, *J. Climate*, 30, 7157–7168, doi:10.1175/JCLI-D-16-0877.1.

### Other papers

Nilsen T., K. Rypdal, and H.-B. Fredriksen (2016), **Are there multiple scaling regimes in Holocene temperature records?**, *Earth syst. dyn.*, 7, 419–439, doi:10.5194/esd-7-419-2016.

### Other publications and presentations

#### As first author

Fredriksen, H.-B., and M. Rypdal, Global surface temperature response explained by multi-box energy balance models. Oral presentation at *CHESS All Staff Meeting*, Bergen, March 2017.

Fredriksen, H.-B., M. Rypdal, and K. Rypdal, Scaling of temperatures produced by linear energy balance models. Oral presentation at *CVAS workshop*, Hamburg, November 2016.

Fredriksen, H.-B., and M. Rypdal, Global surface temperature response explained by multi-box energy balance models. Poster presentation at *American Geophysical Union Fall Meeting*, San Francisco, December 2016.

Fredriksen, H.-B., M. Rypdal, and K. Rypdal, How can long-range memory in surface temperatures be produced?. Oral presentation at *ResClim All Staff Meeting*, Bergen, March 2016.

Fredriksen, H.-B., M. Rypdal, and K. Rypdal, The potential of explaining low-frequency temperature variability by a linear model. Oral presentation at *European geosciences union general assembly*, Vienna, April 2016.

Fredriksen, H.-B., K. Rypdal, and M. Rypdal, Spatiotemporal variability of instrumental and climate model surface temperatures. Oral presentation at *Scales and scaling in the climate system: bridging theory, climate models and data*, Montreal, October 2015.

Fredriksen, H.-B., O. Løvsletten, M. Rypdal, and K. Rypdal, The statistical differences between the gridded temperature datasets, and their implications for stochastic modelling. Poster presentation at *Resclim All Staff Meeting*, Hurtigruten, March 2015.

Fredriksen, H.-B., K. Rypdal, and M. Rypdal, Spatiotemporal correlation structure of the Earth's surface temperature. Poster presentation at *European geosciences union general assembly*, Vienna, April 2015.

Fredriksen, H.-B., En investering i tvil. *Nordlys*, 30.07.2015.

Fredriksen, H.-B., Eilertsen-bløffen. *Nordlys*, 27.06.2015.

Fredriksen, H.-B., K. Rypdal, and M. Rypdal, Why does global surface temperature exhibit more persistent temporal scaling than local temperatures?. Poster presentation at *European geosciences union general assembly*, Vienna, April-May 2014.

Fredriksen, H.-B., O. Løvsletten, M. Rypdal, and K. Rypdal, The statistical differ-

ences between the gridded temperature datasets, and their implications for stochastic modelling. Poster presentation at *American geophysical union fall meeting*, San Fransisco, December 2014.

Fredriksen, H.-B., K. Rypdal, and M. Rypdal, Long-range memory in Earth surface temperature: spatial scale dependence and land-sea differences. Poster presentation at *European Geosciences Union General assembly*, Vienna, April 2013.

Fredriksen, H.-B., K. Rypdal, M. Rypdal, and O. Løvsletten, Spatial scale dependence of long-range memory properties of Earth surface temperature. Poster presentation at *American Geophysical Union Fall Meeting*, San Fransisco, December 2013.

**As co-author**

Rypdal M., E. B. Myklebust, K. Rypdal, H.-B. Fredriksen, O. Løvsletten, and T. Nilsen, Early-warning signals for tipping points in strongly driven systems with many characteristic time scales. Oral presentation at *CRITICS Workshop*, Kulhuse, Denmark, September 2016.

Nilsen, T., K. Rypdal, H.-B. Fredriksen, and D. V. Divine, Is there a break in scaling on centennial time scales in Holocene temperature records?. Poster presentation at *International Partnerships in Ice Core Sciences (IPICS) second open science conference*, Hobart, Tasmania, March 2016.

Løvsletten, O., M. Rypdal, K. Rypdal, and H.-B. Fredriksen, Statistics of regional surface temperatures post year 1900. Long-range versus short-range dependence, and significance of warming trends. Poster presentation at *European Geosciences Union General Assembly*, Vienna, April 2015.

Nilsen T., K. Rypdal, and H.-B. Fredriksen. Little evidence for multiple scaling regimes in Holocene surface temperatures. Oral presentation at *Scales and scaling in the climate system: bridging theory, climate models and data*, Montreal, October 2015.

Rypdal K., M. Rypdal, and H.-B. Fredriksen, Spatiotemporal correlations in Earth's temperature field from fractional stochastic-diffusive energy balance models. Oral presentation at *European geosciences union general assembly*, Vienna, April 2015.

Nilsen, T., H.-B. Fredriksen, and K. Rypdal, Long-range memory in temperature

reconstructions from ice cores: glacial vs interglacial climate conditions. Poster presentation at *ResCLIM All Staff Meeting*, Hurtigruten, March 2015.

Rypdal M., K. Rypdal, and H.-B. Fredriksen, Are the scaling properties of instrumental and long-term proxy temperature records consistent with a simple energy balance model?. Poster presentation at *European geosciences union general assembly*, Vienna, April 2015.

Nilsen T., K. Rypdal, H.-B. Fredriksen, M. Rypdal, and O. Løvsletten, Is there a break in scaling on centennial time scale in Holocene temperature records. Oral presentation at *European geosciences union general assembly*, Vienna, April 2015.

Solhaug, R. M., T. Nilsen, Fredriksen H.-B., Rypdal K., C. Hall, Hvorfor skal vi stole på klimaforskerne? *Labyrint*, 2014.

Løvsletten O., M. Rypdal, K. Rypdal, and H.-B. Fredriksen, Significance-testing of trends: Long-range dependence and model selection. Oral presentation at *Physical origins of correlated extreme events*, Dresden, Germany, June 2014.

Rypdal K., M. Rypdal, T. Nilsen, and H.-B. Fredriksen, The Nature of the Macroweather-Climate Scaling Break in the Holocene. Oral presentation at *American Geophysical Union Fall Meeting*, San Fransisco, December 2014.

Nilsen T., H.-B Fredriksen, K. and Rypdal, Long-range memory in temperature reconstructions from ice cores: glacial vs interglacial climate conditions. Poster presentation at *American Geophysical Union Fall Meeting*, San Fransisco, December 2014.

# Chapter 2

# Simple climate models

To understand global temperature change, a simple climate model is sufficient – if more energy goes into the climate system than out, the total energy and hence the global temperature must change. To go into more detail on how the temperature changes locally and to study other processes we do of course need to add more complexity to the model, which is why we have developed a wide range of model complexities, from Simple Climate Models (SCMs), through Earth System Models of Intermediate Complexity (EMICs) and up to the most sophisticated Earth system models (ESMs). This chapter will discuss various simple climate models, and how models with LRD fit into this framework.

## 2.1 Models for global temperature

### 2.1.1 Energy balance models

The rate of change of energy, and hence temperature, is determined by the difference between energy going in and energy going out of the climate system;

$$\frac{dQ}{dt} = E_{\text{in}} - E_{\text{out}} \tag{2.1}$$

where $E_{\text{in}}$ is determined by the amount of solar radiation reaching the Earth and what fraction of it that is absorbed. $E_{\text{out}}$ is the energy emitted by the Earth. If the Earth was a perfect black body it follows from Stefan-Boltzmann's law that $E_{\text{out}} = \sigma T^4$. This is a good description if $T$ is the temperature at the point in the atmosphere where radiation can freely escape to space, but this temperature is lower than at the surface. If letting $T$ denote the surface temperature, $E_{\text{out}}$ can be approximated by $\epsilon\sigma T^4$, where the *emissivity* $\epsilon < 1$ accounts for greenhouse gases in the atmosphere. An alternative approximation $E_{\text{out}} = A + BT$ was proposed by

Budyko (1969) and Sellers (1969). When we have energy balance, we can find a stable equilibrium state close to today's temperature, but other states also exist. Some hundred million years ago, the Earth was in a state with a temperature so low that oceans were frozen to a depth of several kilometers.

If we linearize the temperature perturbation around today's equilibrium state, the energy balance model reduces to

$$\frac{dQ}{dt} = N(t) = -\lambda\, \Delta T(t) + F(t) \tag{2.2}$$

where the forcing $F(t)$ represents radiative perturbations to the equilibrium state we linearized around, $-\lambda\Delta T(t)$ the Earth's adjustment to this perturbation, and $N(t)$ is the net energy imbalance. The time it takes to adjust the temperature to a new equilibrium temperature $\Delta T_{\text{eq}} = F/\lambda$ depends on $\lambda$ and how $\frac{dQ}{dt}$ relates to $\frac{d\Delta T}{dt}$.

The simplest way to express a change of the energy content is $\Delta Q = C\Delta T$, where $C$ is the average heat capacity of Earth's surface. This results in what we call the one-box model, which is a single ordinary differential equation (ODE) for $\Delta T$

$$C\frac{d\Delta T}{dt} = -\lambda\, \Delta T(t) + F(t) \tag{2.3}$$

For this model to fit well with the temperature change we observe, $C$ must be the heat capacity of a surface layer with depth approximately corresponding to the mixed layer of the ocean. However, this layer may also exchange heat with the deeper layers of the ocean, so we may also need a term in $\frac{dQ}{dt}$ that describes this energy exchange.

### 2.1.2 Vertical one-dimensional model

One way of including energy exchange with the deep ocean is to add a heat flux $\gamma\Delta T$ down into the deep ocean (Gregory and Mitchell, 1997; Raper et al., 2002). With this term, the deep ocean is treated as a non-interactive reservoir, and the form of Eq. (2.3) remains the same. If we are interested in the temperature response on centennial time scales, the deep ocean is also responding, and should be treated as an interactive part that can also have an impact on the heat uptake. It could for instance be included in the model by letting the heat exchange take the form $\kappa(\Delta T_1 - \Delta T_2)$, where $\Delta T_1$ and $\Delta T_2$ correspond to the temperature changes in the upper and deeper layer of the ocean. Then we also need an equation describing the

temperature evolution of the deep ocean, resulting in a system of coupled ODEs:

$$C_1 \frac{d\Delta T_1}{dt} = -\lambda\ \Delta T_1 + \kappa(\Delta T_1 - \Delta T_2) + F(t)$$
$$C_2 \frac{d\Delta T_2}{dt} = -\kappa(\Delta T_1 - \Delta T_2)$$

This two-box model has been studied by various authors (Held et al., 2010; Rypdal, 2012), and found to fit well with the long-term global temperature response seen in complex climate models (Geoffroy et al., 2013). Some also included an atmospheric box in addition to these two ocean boxes (Grieser and Schönwiese, 2001; Dickinson, 1981). The surface temperature response resulting from a linear system of coupled ODEs is given by a sum of exponential responses to the forcing, whose time scales are minus the inverse of the real part of the eigenvalues of the linear system. Furthermore, the ocean can also be split up into even more boxes, resulting in additional time scales, e.g. like in Fredriksen and Rypdal (2017) and Li and Jarvis (2009).

An alternative to describing the vertical structure of the ocean as boxes is to use a continuous model. The simplest continuous models describe transport as heat conduction, resulting in a diffusion model (Lemke, 1977; Fraedrich et al., 2004). The diffusion model is not meant to describe a purely diffusive transport, but is rather a parametrization of more complex turbulent processes that lead to a transport. Some of the diffusion models also include advective terms describing upwelling and downwelling (Hoffert et al., 1980; Meinshausen et al., 2011), resulting in a simplified model for ocean circulation, where water is upwelling across the world ocean and returning to the deep ocean by downwelling in polar areas.

The net global effect of upwelling and downwelling is estimated by Hoffert et al. (1980) to be an upwelling velocity of 4 m/yr, taking into account that the upwelling happens over a much larger area than the downwelling. The resulting equation for the global mean potential temperature is the upwelling-diffusion equation

$$\frac{\partial T}{\partial t} = K\frac{\partial^2 T}{\partial z^2} + w\frac{\partial T}{\partial z} \tag{2.4}$$

They also find that the stationary vertical profile of the potential temperature

$$T(z) = T_0 + T_1 e^{-z/z^*} \tag{2.5}$$

well describes observations, with a characteristic depth $z^*$ of the temperature profile. This model can successfully reproduce the surface temperature change in the atmosphere-ocean general circulation model (AOGCM) HADCM2 under different forcing scenarios (Raper and Cubasch, 1996; Raper et al., 2001). The structure of the heat uptake of the deeper ocean is not well reproduced though. Furthermore,

Gregory (2000) criticizes the use of this simplified model as a physical explanation of the heat uptake during climate changes. He finds that in HADCM2, the majority of the heat exchange happens in the Southern Ocean, where the advective processes transport heat downwards and diffusive processes transport heat upwards. These processes are the reverse of what is assumed in the global upwelling-diffusion model.

Because of the reduced computing time of the simple models, and their assumed realistic surface temperature response, they have been widely used by the IPCC. When tuned to complex models, many quick realizations emulating the complex models can be produced. This provides important sources for uncertainty estimation and for making long future projections. In the latest report (IPCC, 2013), the MAGICC model is used (Meinshausen et al., 2011). This is an upwelling-diffusion model that includes downwelling in polar areas, separate between the two hemispheres and between land and ocean, in addition to including a simple carbon cycle.

When discretizing a continuous model, as is often done in numerical solutions, it practically becomes a multibox model. If we let the heat capacity of each box be along the diagonal in the diagonal matrix $\mathbf{C}$, and temperature changes in the different boxes are collected into the vector $\mathbf{\Delta T}$, we may describe the temperature change as

$$\mathbf{C}\frac{d\mathbf{\Delta T}}{dt} = \mathbf{H}(\mathbf{\Delta T}, t) + \mathbf{F}(t) \tag{2.6}$$

where the forcing $\mathbf{F}(t)$ acts on all surface boxes, and $\mathbf{H}$ may in general be a vector of nonlinear functions. To get a very accurate representation of reality, other variables than temperature may also have to be included in the system of equations. Our goal, however, is to find a simple representation that can describe the temperature evolution with reasonable accuracy. So from this general system, we make the simplification that the temperature changes can be parametrized only in terms of a forcing and a linear function of other temperature changes in the system, such that we may write this as a linear system

$$\mathbf{C}\frac{d\mathbf{\Delta T}}{dt} = \mathbf{A}\mathbf{\Delta T} + \mathbf{F}(t) \tag{2.7}$$

where the matrix $\mathbf{A}$ contains coefficients $A_{ij}$ that determine the mean interaction between box $i$ and $j$ in the system on the time scales of interest. In a diffusion model where the boxes are aligned vertically, the matrix $\mathbf{A}$ is tridiagonal because we only include dependence on the box above or below. This is the case in the 3-box model studied in Fredriksen and Rypdal (2017), but note that any linear interaction between two boxes could be included, for instance to model upwelling and downwelling. That would result in a less sparse matrix, but in all cases where $\mathbf{A}$ can be diagonalized, the solution is given by a sum of exponential responses

convolved with the forcing. The surface temperature in a system of $N$ boxes can thus be given by:

$$\Delta T(t) = \int_{-\infty}^{t} \sum_{k=1}^{N} b_k e^{-(t-s)/\tau_k} F(s) ds \tag{2.8}$$

where $\lambda_k = -1/\tau_k$ are the eigenvalues of $\mathbf{A}$. In the other boxes we have solutions on the same form, just with other values of $b_k$. The general form of the response function means that there may also be different matrices giving rise to the same response function, that is, different choices of ocean dynamics may result in the same surface temperature response. Hence the response function in Fredriksen and Rypdal (2017) is more general than the physics we derived it from, and the translation into parameters $C_i$ and $\kappa_i$ describing heat capacities and heat conductivities should be considered an example of how the physics behind the response can be parametrized. To determine the most correct physical model of surface temperature response, it is necessary to also consider the temperature change in the deeper parts of the ocean.

### 2.1.3 Impulse response models

The sum of exponential Green's function in Eq. (2.8) may be generalized to be any Green's function $G$:

$$\Delta T(t) = \int^{t} G(t-s) F(s) ds \tag{2.9}$$

The corresponding differential equation can be written as

$$\mathcal{L}_t \Delta T(t) = F(t) \tag{2.10}$$

where $\mathcal{L}_t$ is the linear differential operator corresponding to the Green's function $G(t)$.

By making this generalization, it may be harder to keep track of the physical interpretation of $\mathcal{L}_t$, but it may still result in a valuable tool if the amount of parameters that needs to be estimated from data is reduced. When determining a suitable Green's function, idealistic forcing scenarios are commonly used, such that the shape of the response can be seen as clearly as possible. Complex climate models are often forced by an instant doubling or quadrupling of the $CO_2$ concentration, implying that $F(t)$ is a step-function and the temperature response is just the integral of the Green's function. A suitable function can then be fitted to the temperature response to determine the parameters in the model. Alternatively, one can compute a Green's function only determined by data, without any parameters (Good et al., 2011; Hansen et al., 2011; Ragone et al., 2015; Lucarini

et al., 2016). Unless smoothed or ensemble averaged, such a Green's function will look noisy due to the influence from internal fluctuations.

Several Green's functions have been suggested for describing the temperature response (Rypdal, 2012), and it has been demonstrated that the choice impacts attribution studies (Rypdal, 2015). It is also crucial for future projections of temperature how strong the delayed responses are. The power-law response studied by Rypdal (2012) and Rypdal and Rypdal (2014) implies that that the delayed responses will be important, resulting in a continued temperature rise for a long time, even if we kept the forcing level constant from now on.

When making temperature projections for the next century, it was previously common to prescribe the concentration of $CO_2$ and let the climate models compute the temperature response to that. In todays ESMs, a carbon cycle is often included as an interactive part, so the emission scenarios are prescribed, and the model computes both the $CO_2$ concentration and the following temperature response. The relation between emissions and atmospheric concentration is determined by how fast carbon is removed from the atmosphere, and can also be expressed as a response model. Just as for the temperature, there may be multiple time scales involved in this response – the biological processes on land could for instance respond on a quite different scale than carbon transport to the deep ocean. Linear impulse response models could possibly provide good approximations to these perturbations in $CO_2$ concentration (Hasselmann et al., 1997; K. Rypdal, 2016). The response functions for $CO_2$ used by Hasselmann et al. (1997), Joos et al. (2013) and Meinshausen et al. (2011) consist of a sum of exponential responses, which for suitable choices of the parameters, may be close to the power-law response suggested by K. Rypdal (2016).

### 2.1.4 Stochastic models

The forcing term in the expressions above does not necessarily include only deterministic forcings, like solar, aerosol, and greenhouse gases. It can also include a stochastic part. The stochastic forcing is often taken to be a white noise (e.g. like in Rypdal and Rypdal (2014), Fredriksen and Rypdal (2017)), and the response to this is meant to describe internal fluctuations in the temperature.

Stochastic climate modelling was first introduced by Hasselmann (1976). The idea was that we have a set of hydrodynamic equations, where $u_i$ and $v_i$ are in

general nonlinear functions,

$$\frac{dx_i}{dt} = u_i(\mathbf{x}, \mathbf{y}) \tag{2.11}$$

$$\frac{dy_i}{dt} = v_i(\mathbf{x}, \mathbf{y}) \tag{2.12}$$

$$\tag{2.13}$$

The variables $x_i$ describe fast processes like weather, and the variables $y_i$ describe slow climatic variables such as sea surface temperature, ice coverage, etc., that are constants in a weather model. The time-scale separation between the climate and weather variables ($\tau_y >> \tau_x$) allows us to reduce this system to

$$\frac{dy_i}{dt} = \langle v_i(\mathbf{x}, \mathbf{y}) \rangle + v_i' \tag{2.14}$$

where $v_i' = v_i(\mathbf{x}, \mathbf{y}) - \langle v_i \rangle$, and the angle brackets denote ensemble average over the variables $\mathbf{x}$ for a fixed $\mathbf{y_0}$. According to Hasselmann (1976), the time-scale separation *enables statistical closure through the application of the Central Limit Theorem, whereby the response of a system is completely determined statistically by the second moments of the input if the forcing consists of a superposition of a large number of small, statistically independent pulses of time scale short compared with the response time of the system.* Hence, we may think of internal surface temperature fluctuations on climatic scales as one of the variables $y_i$ that is being driven by the stochastic weather variability $v_i'$. If we approximate $\langle v_i(\mathbf{x}, \mathbf{y}) \rangle$ as a linear function of $\mathbf{y}$, and we model the weather fluctuations as a white noise/increments of a Brownian motion ($dB$), the temperature response is a linear response to the weather forcing:

$$\Delta T(t) = \int^t G(t-s) dB(s). \tag{2.15}$$

This is similar to the deterministic response in Eq. (2.9), except that we now have a stochastic integral.

If the surface temperature was disconnected from all other climate variables, we could consider the solution to that single equation, resulting in an exponential Green's function, and a $\Delta T$ that is an OU process. Or alternatively discretized to an autoregressive process of order 1 (AR(1)). AR(1) is a commonly used model for internal temperature fluctuations, likely because it is the simplest stochastic model with memory, but we should keep in mind that it neglects all interaction between climate variables. When the surface temperature equation is linearly dependent on other climate variables, e.g. deeper ocean temperatures as discussed before, the internal variability is instead a multivariate AR(1) process. The surface temperature response is thus a sum of exponential responses to the white noise

forcing, which becomes a sum of AR(1) processes. If this sum is such that it can be well approximated by a power-law response, it can instead be modelled as a long-memory process.

Examples of long-memory processes are the fractional Gaussian noise (fGn) and the fractionally integrated autoregressive moving average (FARIMA) process. These processes are mathematically very similar, and are characterized by the asymptotic power-law tail of the ACF: $C(\tau) \approx \tau^{-\alpha}$ and corresponding power-law PSD: $S(f) \propto f^{-\beta}$. One way of formulating a long-memory process is, although mathematically not well defined (Rypdal and Rypdal, 2014),

$$X_{\mathrm{fGn}}(t) = \int_{-\infty}^{t} (t-s)^{\beta/2-1} dB(s) \tag{2.16}$$

We note from this that any point in the process is dependent on all past points of $dB$, but this infinitely long memory should be considered a mathematical idealization that could be cut off at some point. Cutting the memory is necessary for the system to conserve energy. But for practical purposes, it will not make a big difference if the memory is cut or not, as long as we cut on a long enough time scale. So even though a process like an fGn in theory is unphysical, it can be considered a good approximation to the multi-scale processes in the climate system. The main advantage of using this approximation is the reduction in the number of parameters, compared to using a full multivariate autoregressive process that describe all important mechanisms. With many free parameters, a multivariate process may produce a reasonable response function with several different choices of the parameters, and it can therefore be difficult to know if we have the most physically correct parameters without observation data for all other mechanisms.

Figure 2.1 shows an example of both a single OU process and an fGn. The OU process in (a) shows variability with a characteristic time scale of $\tau = 4.3$ years, while the fGn in (c) includes variability on both longer and shorter scales. The time scales of variability become more apparent when studying the PSDs in (b) and (d). The expected PSD of an OU process is

$$S(f) \propto \frac{1}{(2\pi f)^2 + (1/\tau)^2}, \tag{2.17}$$

and is shown by the black curve in the figure. We note that this spectrum has a characteristic mode when the two terms in the denominator are of the same size, that is, at frequency $f \approx 1/(2\pi\tau)$. At lower frequencies, the spectrum becomes constant/white, and at higher frequencies we have $S(f) \propto 1/f^2$. The parameters used are estimated by Rypdal and Rypdal (2014) with a maximum likelihood routine, which finds the Green's function that best describe both deterministic and stochastic part of global temperature simultaneously. The resulting time scale

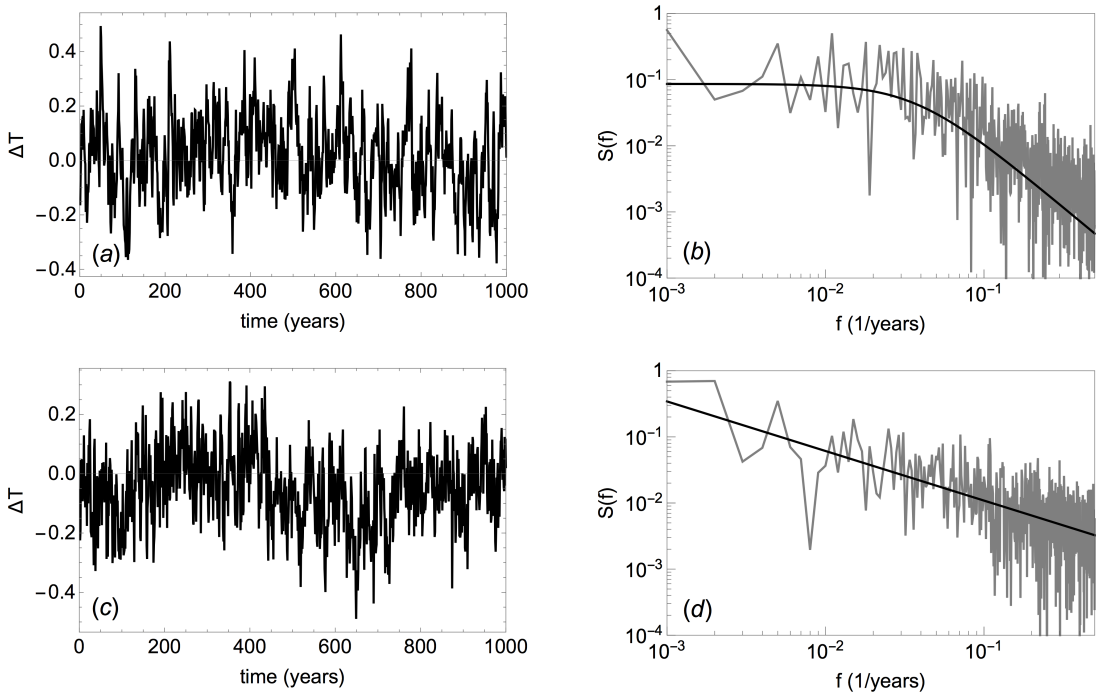


**Figure 2.1:** Examples of stochastic models for temperature, generated with the parameters estimated for global temperature by Rypdal and Rypdal (2014). (a) Realization of an OU process with time scale $\tau = 4.3$ years and standard deviation $\sigma_T = 0.15$. In (b) the gray curve is the periodogram of the time series in (a) and the black curve is the expected PSD of this process. (c) Realization of an fGn with $\beta = 0.75$ and $\sigma_T = 0.13$, and (d) is the estimated and expected PSD of (c).

of 4.3 years is consistent with the response time of the mixed layer in the ocean. In Figure 2.1(b) we observe that this corresponds to a a characteristic mode in the spectrum of the stochastic part around the frequency $f \approx 1/(2\pi \cdot 4.3)$ yr$^{-1} \approx 1/27$ yr$^{-1}$. Hence the information we have about the periods of the PSD is zoomed in a factor of $2\pi$ compared to the response times observed in the time domain. This means that if we have information about e.g. a deep ocean response time of about a few centuries, the corresponding mode in the spectrum will be seen at a millennial scale.

The introduction of stochastic climate models by Hasselmann (1976) was part of a series of papers, followed by a paper by Lemke (1977) who studied examples of such models. The models included mechanisms for heat exchange with the deeper oceans, leading to spectra remarkably close to power laws for frequencies higher than $f \approx 1/100$ yr$^{-1}$. This paper provides an early demonstration of how power-law spectra on scales from months to centuries can arise. The notion of long-range

dependence of temperature fluctuations and associated use of fGns as statistical temperature models became known much later though, around mid-90s.

## 2.2 Spatially dependent models

So far I have discussed models for global temperature, called zero-dimensional models since there are no spatial coordinates, and one-dimensional models with one spatial coordinate for the vertical ocean column. In other one-dimensional climate models, the only spatial coordinate is the latitude. Papers studying these models are Budyko (1969) and Sellers (1969). In one-dimensional models with no vertical coordinate, we consider only a surface layer with average heat capacity $C$, and the heat uptake per unit area could be described by

$$C\frac{\partial T}{\partial t} = (E_{\text{in}} - E_{\text{out}}) + D\frac{\partial}{\partial y}(1-y^2)\frac{\partial T}{\partial y}, \tag{2.18}$$

where $y \in (0,1)$ is the cosine of the polar angle $\theta \in (-\pi/2, \pi/2)$. The incoming energy will now depend on latitude due to the higher albedo at high latitudes, and the last term is a poleward heat transport described mathematically as a diffusion term. In reality this transport is due to ocean currents, large convective cells and turbulent transport in the atmosphere.

By including a zonal coordinate, we obtain a two-dimensional model, for instance as in North et al. (2011):

$$C\frac{\partial T}{\partial t} = -BT + D\nabla^2 T + BF(x,y,t), \tag{2.19}$$

where $T$ is the temperature anomaly at a point on the surface. $B$ is the feedback parameter, $D\nabla^2 T$ is horizontal diffusion, and $F(x,y,t)$ is the forcing. North and coworkers have published papers on similar models over several decades, some studying the response to deterministic forcing (Kim et al., 1992), and others focusing on the statistical properties of stochastically forced models (North and Cahalan, 1981; Kim and North, 1991, 1992). A review of these and other EBMs in the literature until 1981 is found in North et al. (1981).

Some of these models include interaction with a deep ocean (e.g. Kim and North (1992)), while others consider only a surface layer (Kim and North, 1991; North et al., 2011). In the former case Kim and North (1992) present spectra with a $1/f$ shape, while in the latter case, the temporal characteristics are analogous of an AR(1) process. By modifying the response in North et al. (2011), Rypdal et al. (2015) obtained a model with power-law spectra for both local and global temperatures. This model has only horizontal spatial coordinates, but we can

think of it as also indirectly including a vertical dimension whose impact is baked into the power-law response.

This model can well describe the average characteristics of surface temperature fluctuations, but assumes a uniform Earth and does not model the spatial differences of the characteristic variability. We observe for instance large differences between land and sea, and between tropics and mid/high latitudes (Fredriksen and Rypdal, 2016).

## 2.3 Linearity, feedbacks and sensitivity

Linearity of a model implies that the temperature response to a combination of different forcing agents can be split up into a sum of the response to each of them. This hypothesis has been tested for several models, and is found to be good for both GCMs (Meehl et al., 2004; Geoffroy et al., 2013) and for EMICs (Eby et al., 2013). Even though climate processes contain nonlinearities, a linear approximation is desirable due to the great simplifications made if the contributions from the nonlinear parts of the response are small enough to be neglected. To check if the response is best described as linear or nonlinear, the only well-posed scientific hypothesis we can formulate is that the response is linear (K. Rypdal and M. Rypdal, 2016). The reason is that the linearity hypothesis is falsifiable, contrary to the hypothesis of a nonlinear response. The latter is however verified if the linearity hypothesis is falsified.

The linearity hypothesis has been used quite extensively without being falsified, and is therefore likely to be a good description of the temperature response. Just as a linear function can be a good approximation to any continuous function within some range, it may not be surprising that a linear temperature response can be a good approximation to the full response in a certain range. Hence the question that needs to be answered is rather in what range is a linear response a good approximation?

Hasselmann et al. (1993, 1997) argues that linearity of the response may only be valid up to a doubling of $CO_2$, corresponding to a temperature change up to 3C. They claim this limitation is due to the *temperature feedback on the $CO_2$ model (increasing temperature decreases the $CO_2$ solubility of sea-water and thus increases the atmospheric retention factor).* To go beyond this range Hooss et al. (2001) suggested a nonlinear extension of the impulse response model through explicit treatment of what they consider to be the climate system's dominant nonlinearities: $CO_2$ chemistry in ocean water, $CO_2$ fertilization of land biota, and sublinear radiative forcing.

Step-forcing experiments like sudden doubling or quadrupling of the $CO_2$ concentration are commonly used to find the linear response function though (Hansen

et al., 2011; Geoffroy et al., 2013; Proistosescu and Huybers, 2017), with seemingly successful results. Perhaps because $CO_2$ is prescribed rather than being an interactive part of the model. Processes resulting in important nonlinear responses may not even be captured properly by the ESMs. In addition to the nonlinearities mentioned by Hooss et al. (2001), tipping points, like a shutdown of the overturning circulation, ice sheet collapses, etc. are examples of nonlinear responses relevant for future climate states. Knowledge of such processes far beyond our current climate state are difficult to model, as the only data we have about them are paleodata, with high uncertainty.

In the global energy balance model Eq. (2.2) we assumed a constant feedback parameter. This assumption has been tested using data from climate models with constant forcing to plot $N(t)$ vs. $\Delta T(t)$, a so-called Gregory plot, after Gregory et al. (2004). $\lambda$ can be found by making a linear fit to these data, but for many models a linear fit is poor (Andrews et al., 2012, 2015; Armour, 2017). The equilibrium climate sensitivity is the reciprocal of $\lambda$, and is found to increase with time/timescale. This non-constancy of the climate feedbacks are often associated with non-linear behaviour (Good et al., 2011). However, it does not necessarily imply nonlinear feedbacks if the time dependence arises from a spatial dependence of the feedback parameter (Armour et al., 2013).

Proistosescu and Huybers (2017) suggest a linear response model for global temperature consisting of three exponential responses, and decompose the radiative response in the same way. The proportionality factor between each mode of the radiative response and temperature response becomes a distinct feedback parameter for each characteristic time scale. With this time-scale dependent feedback parameter they are able to explain the nonlinear relation between the top-of-atmosphere energy flux and the global temperature. For our three-box model (Fredriksen and Rypdal, 2017) to be consistent with this we can choose three boxes connected to the surface instead of being vertically aligned.

Having several boxes connected to the surface results in a mathematically similar response function for global temperature, as having boxes aligned vertically. But if we require a time-scale dependent radiative response that is still restricted to the linear feedback assumption, we need several boxes in the surface layer with distinct feedback parameters. In this case, the radiative response in the energy balance equation for global temperature may not be well approximated as a linear function of global temperature, that is, the approximation $\sum_k f_k \lambda_k \Delta T_k \approx \lambda_G \Delta T_G$ may not hold. Here $f_k$ is the fraction of the surface covered by box $k$, with temperature $\Delta T_k$ and feedback parameter $\lambda_k$. The subscript $G$ refers to globally averaged quantities. Despite the time-scale/spatial dependence of the linear feedback parameter, we note that the global temperature response could still be described in terms of one linear response model consisting of a superposition of different modes.

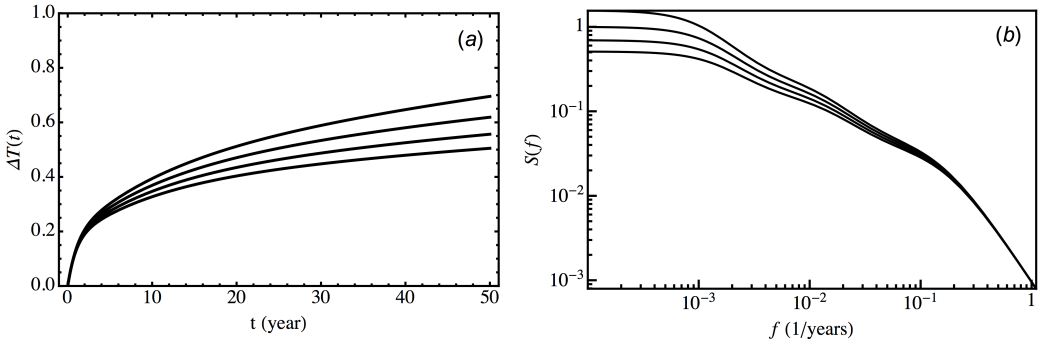


**Figure 2.2:** The effect of changing the feedback parameter while keeping all other parameters constant. The other model parameters are as estimated for global temperature on time scales 1, 10 and 100 years in paper III, and the set of feedback parameters used for these four curves is (0.8, 1.0, 1.2, 1.4).

The only example of a spatially dependent $\lambda$ used by Fredriksen and Rypdal (2017), is the distinction between land and sea surface. We find that with our two different feedback parameters for land (L) and ocean (O), the global radiative response can be very well approximated as proportional to the global temperature, $f_L\lambda_L\Delta T_L + f_O\lambda_O\Delta T_O \approx \lambda_G\Delta T_G$. Hence, our results suggest that the box configuration resulting in $\sum_k f_k\lambda_k\Delta T_k \not\approx \lambda_G\Delta T_G$ might instead be found within the ocean surface, consistent with the findings of the slow warming in the Eastern Equatorial Pacific and Southern Ocean being the primary reason of the time-dependence of the sensitivity (Proistosescu and Huybers, 2017).

Part of the spatial dependence of $\lambda$ could be due to the different atmospheric feedback mechanisms in different regions, while other parts of the spatial dependence could arise due to a time-scale dependence of $\lambda$. The latter becomes apparent due to differences in mixing processes of the water, resulting in differences in effective thermal inertia and time scales of response. Thus, in regions dominated by slow responses, long-term feedbacks will be weighted more in the linear regression between radiative response and temperature response. This spatial variation of response times may also be related to the findings that the time-varying $\lambda$ is caused by evolving spatial patterns of warming (Andrews et al., 2015). It may also explain why feedback parameters determined by regression between $N$ and $T$ for internal variability differ from feedback parameters determined from forced responses, since the patterns of internal temperature change could differ from those of forced changes (see Gregory and Andrews (2016) and references therein).

Since $\lambda$ is often observed to be changing with time, and in addition varying among models, it is useful to take a closer look into how different $\lambda$'s affect the response function. We will also look into how the internal variability can be

affected, assuming it is generated by the same response function. Figure 2.2 (a) shows the response function for a unit-step forcing for four different values of $\lambda$. The highest value of $\lambda$ corresponds to the lowest value of the climate sensitivity, and hence the bottom curve. Also in the spectrum of the stochastic part in (b), the highest value of $\lambda$ corresponds to the bottom curve. From this spectrum we observe that a variation of $\lambda$ leads to a change in the slope of the spectrum, but probably only detectable above centennial scales.

The response functions plotted in Figure 2.2 (a) have a slower response for the first $\approx$ 40 years than the CMIP5 step responses plotted in Fredriksen and Rypdal (2017). Low transient responses in observation data could be a result of low data coverage in certain areas (Richardson et al., 2016), particularly in polar areas, where climate models show amplified responses. Currently, that is my main hypothesis for the discrepancy between CMIP5 step responses and our estimated step response, although some other hypotheses were also suggested in Fredriksen and Rypdal (2017).

Hansen et al. (2011) on the other hand, suggest that climate models mix heat too fast, and hence respond too slowly. This may seem contradicting to our results of an initially weaker response in observations than models. However, if normalizing the CMIP5 response functions plotted in Fredriksen and Rypdal (2017) by their climate sensitivity, the resulting step responses are higher than the slowly responding climate model shown in Figure 5 of Hansen et al. (2011). They are more comparable to their suggested intermediate response in the same figure.

We must however keep in mind that response functions showing fractions of new equilibrium temperature also depend on the climate sensitivity, even though they are normalized, and interpretations of these plots must be done with care. Figure 2.3 demonstrates what happens if the responses plotted in Figure 2.2 are normalized by their climate sensitivity. In this plot the lower values of the response are only due to a higher sensitivity. The estimated values of climate sensitivity are therefore also a possible explanation of why the CMIP5 step-responses with parameters from Geoffroy et al. (2013) differ from the estimated model response in Hansen et al. (2011).

The issues with the large uncertainty of the climate sensitivity, and a possible time variation, could hopefully be better constrained in the future as we get more and better observations of ocean heat uptake and energy imbalance on top of the atmosphere.

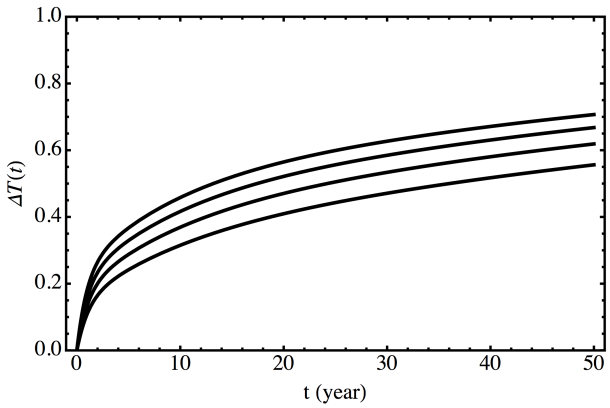


**Figure 2.3:** The responses in Figure 2.2 normalized by their equilibrium climate sensitivity. The response with the highest sensitivity is now the bottom curve.

# Chapter 3

# Long-range dependence in surface temperatures

No known physical principles imply that we can expect scale invariance in the climate system. It is hence no reason to make this assumption about the temperatures *a priori*. It is rather something we can infer after analyzing the temperature fluctuations for a limited range of time scales, and is just an approximation to more complex dynamics.

## 3.1 Motivation

Let us start by looking into the motivation for studying LRD in temperatures. The first geophysical quantity observed to have this property was the discharges of the river Nile analyzed by Hurst (1951) and Hurst et al. (1965). Hurst (1951) also mentioned a few other geophysical examples, followed by even more by Mandelbrot and Wallis (1969). One of the reasons this property is particularly interesting, is that it implies an infinitely long dependence between the values of a time series. In addition it is connected to fractals or self-similarity, that is, if we zoom in or out on the time series and maybe stretch it in one direction, we will observe the same structure as originally. Mandelbrot and Van Ness (1968) proposed the fractional Gaussian noise (fGn) that could be used to model this phenomenon.

According to Mandelbrot and Wallis (1969), another significance of the so-called Hurst's law in geophysics, is that it may wipe out the distinctions between fields studying atmospheric fluctuations on different scales: turbulence (seconds - minutes), meteorology (days - weeks), macrometeorologists (a few years), climatologists (centuries) and paleoclimatologists (>centuries). They think these distinctions are similar to classifying bits of rock into sand, pebbles, and stones.

## 3.2 Observations

Some of the first studies of instrumental temperatures in this context were done by Bodri (1994, 1995). A few years before this, Fluegeman and Snow (1989) performed a similar study of an oxygen isotope record from a Pacific sediment core. They found that on a time span from millennia to two million years, this temperature proxy is fractal. Further, they suggested that if the Hurst exponent (or fractal dimension) of temperatures on these long scales is the same as found in modern data on shorter scales, we have reason to think that the fluctuations on intermediate time scales could also be described by the same exponent. It could be a nice tool to extrapolate what temperature variability looks like on time scales that are not resolved by a data set.

These first studies of LRD in temperatures were followed by a large amount of studies attempting to see if all temperatures have this property or not, using various methods. And what Hurst exponent (or other related scaling exponent) that best describe the data. Examples include Pelletier (1997); Koscielny-Bunde et al. (1998); Monetti et al. (2003); Blender and Fraedrich (2003); Fraedrich and Blender (2003); Vyushin et al. (2012).

To test if LRD processes like an fGn is the best description of the data, it must also be tested against other stochastic models. Several studies have therefore compared the fGn to an AR(1). These two processes can both be described by two parameters, the overall variance and a measure of the persistence. If testing against other processes we must add a penalty for eventual extra parameters, for instance by applying the Akaike or Bayesian Information Criteria (AIC/BIC). The result of these studies is that in many areas, particularly in mid/high latitudes and globally, temperatures are best described by an fGn, while in some areas they are better described by an AR(1). Most of the temperatures are however somewhere in between these two classes of processes (Vyushin et al., 2012; Løvsletten and Rypdal, 2016).

In studies estimating the Hurst exponent, it is found that the value is not the same everywhere. Although there are large regional differences in the estimates for sea surface temperature, they generally show more persistence than land temperatures, which are close to a white noise (Pelletier, 1997; Monetti et al., 2003; Fraedrich and Blender, 2003; Fredriksen and Rypdal, 2016). It is also found that averaging temperatures over a larger area results in more persistence, because high-frequency fluctuations are averaged out to a larger degree than low-frequency fluctuations, that tend to have a larger spatial extent (Fredriksen and Rypdal, 2016).

In addition to the spatial dependence of the Hurst exponent, a timescale dependence is also observed. Since each time series covers only up to a few orders of

magnitude of time scales, composite spectra consisting of several different records are needed to cover the spectrum at all time scales of interest. Such spectra appear in e.g. Pelletier and Turcotte (1999); Huybers and Curry (2006); Lovejoy and Schertzer (2013). They typically show a power-law behaviour $f^{-\beta}$ with $\beta \approx 2$ on weather scales, and $\beta \in (0, 1)$ for frequencies between 1/100 $\text{yr}^{-1}$ to 1 $\text{yr}^{-1}$, where the value will depend on location and degree of spatial averaging for the record. On frequencies lower than 1/100 $\text{yr}^{-1}$, paleodata typically give $\beta \in (1, 2)$ before the spectra flatten out again on multimillennial scales.

## 3.3 Estimation methods

One characteristic of LRD is the power-law form of the PSD; $S(f) \sim f^{-\beta}$. In a plot with logarithmic axes such a power law is seen as a straight line with slope $-\beta$, which can be estimated using linear regression. In addition to the PSD, there are several other methods that measure the fluctuation level as a function of time scale, which are also applied to assess if time series exhibit LRD. Examples include detrended fluctuation analysis (DFA) (Peng et al., 1994; Kantelhardt et al., 2001), variogram, wavelet variance (Malamud and Turcotte, 1999), etc. Common to them all, is that if we have a time series exhibiting LRD, the fluctuation level $F$ varies with time scale $\tau$ as $F \sim \tau^{\alpha}$. The scaling exponents obtained from the different methods will all be related, and they quantify how persistent the variability is. If applied to a time series that exhibits perfect scaling properties, all the different methods result in similar estimates of the scaling exponent. However, deviations from scaling can result in different outcomes using different methods.

DFA is a particularly popular method for determining scaling exponents, and has been applied in the study of several temperature datasets (Koscielny-Bunde et al., 1998; Blender and Fraedrich, 2003; Rybski et al., 2008; Vyushin et al., 2009). The DFA of order $N$ can remove polynomial trends in a time series up to order $N - 1$. This is particularly useful for studying only the natural part of the variability in instrumental records. DFA also produces a fluctuation function that is quite smooth, so the power-law form becomes more apparent than in noisy estimates of the PSD. To understand why, we will take a look at how it relates to the power spectral density $S_u(\omega)$,

$$F_2[K] = \int_{1/K}^{\pi} \frac{S_u(\omega)}{2(1 - \cos\omega)} d\omega, \tag{3.1}$$

where $K$ is the window size where the fluctuation level is measured (Heneghan and McDarby, 2000). We note that the fluctuation function at time scale $K$ is a weighted sum of the power on all frequencies higher than the frequency corresponding to this time scale. Hence, both the noise and deviations from the power-law

form, are to some degree smoothed out. For instance, in the case where we have a pure sinusoidal signal and get a spike in the spectrum, Hu et al. (2001) show that the fluctuation function flattens out for scales larger than the periodicity of the signal and has a constant steep slope depending on the order of the DFA on small scales. Therefore, DFA has a high spectral leakage compared to the estimates of the spectrum.

DFA is not the only method that produces a smoothed measure of the fluctuation level, actually most of the methods do that to some degree. Fredriksen and Rypdal (2016) performed a log-binning to smooth the periodogram, partly to get rid of the noise, but also because it is desirable to have a measure where all scales are weighted equally when determining the scaling exponent. For the wavelet variance we can have different degrees of smoothing, depending of the choice of mother wavelet. This becomes apparent in Fig. 3.2, where the wavelet variance is computed using both the Mexican hat wavelet and the Morlet wavelet. The wavelet analysis measures the fluctuation level both as a function of time and time scale/frequency, but analogous to the uncertainty principle in quantum mechanics, we cannot have good resolution of both of these quantities simultaneously. A good frequency resolution means poor time resolution and vice versa (Torrence and Compo, 1998).

Contrary to DFA, most of these methods smooth the fluctuation level over a smaller range in frequency-space. The long range of smoothing in DFA may result in conclusions of LRD up to longer scales than is actually the case, or maybe even some false positive conclusions of LRD. It may be a good idea to compare results from different methods before drawing any conclusions.

## 3.4 Different explanations

Suggested explanations of long-range dependence in temperature records focus mostly on time scales from months to centuries, which is also my focus here. By comparing a climate model coupled to the deep ocean to a model that has only a mixed layer, Fraedrich and Blender (2003) find that only the model with the deep ocean coupling can produce LRD on time scales longer than about 15 years. This study suggests therefore that we need the deep ocean to explain the long memory, consistent with other studies demonstrating how simple ocean models can reproduce the observed spectra.

Different types of simple ocean models are discussed in Chapter 2. Older studies, such as Lemke (1977) show the resulting spectra without mentioning the connection to LRD, since this concept was not well known at the time. This connection is only made in more recent studies, as in diffusion models explanations in Pelletier (1997) and Fraedrich et al. (2004), where the atmosphere over an ocean

is inspired by the analogous case of a metallic film over a substrate (van Vliet et al., 1980).

Pelletier (1997) and Pelletier and Turcotte (1999) describe transitions in temperature spectra on all time scales analyzed in terms of diffusion models, even the transition on millennial scales. The latter may be stretching the use of linear models too far, unless extending what we interpret as forcing. The thermal bipolar seesaw model is an example of a possible linear response mechanism between the temperature in the Southern Ocean and North Atlantic (Stocker and Johnsen, 2003), with a characteristic time scale on the order of 1000 years. This equilibration time scale could fit with the observed transition to a white spectrum at millennial scales. However, to describe what forces the large fluctuations observed on these scales we probably need nonlinear responses to temperature changes. For instance are Dansgaard-Oeschger events observed in ice ages associated with changes in ocean circulation and sea ice cover in the North Atlantic (Dokken et al., 2013), which may again depend on temperature changes.

Nonlinear mechanisms are also important on weather scales, and are actually necessary for making the weather equations chaotic, such that weather practically becomes a random process on monthly scales. Alternative hypotheses of the scaling observed on monthly to centennial scales also invoke nonlinear mechanisms. Huybers and Curry (2006) suggest that there could be a nonlinear transfer of energy from the seasonal cycle up to frequencies of $1/100$ yr$^{-1}$, but without specifying the physics. Lovejoy and Schertzer (2013) also suggest a nonlinear mechanism based on an idea that low-frequency weather, or their so-called macroweather, can be explained by a turbulent cascade of energy transfer, similarly as they explain scaling on weather scales. On scales longer than 10-100 years, we have a transition into a steeper spectrum that they call the climate regime. They claim this is due to external climate forcings and new slow climate processes becoming more important (Lovejoy et al., 2013).

In the industrial era the response to anthropogenic forcing results in much more power on frequencies below $1/10$ yr$^{-1}$ than expected from a power law extended from the higher frequencies. And as we will go further into in the following section, during the last ice age we observe a similar increase in the slope of the spectrum below frequencies of about $1/100$ yr$^{-1}$, as a result of a more variable climate state. If we look at proxies that go even further back in time, see e.g. Fig. 1 in Shao and Ditlevsen (2016), we observe that the size of the fluctuations depends on what part of the time series we look at. In contrast, the Holocene temperature fluctuations seem to be quite stationary, that is, we expect to have about the same type of variability at all times throughout the record.

The steeper slope of the spectrum observed for frequencies below $\sim 1/100$ yr$^{-1}$ is a result of a nonstationary process, like a time-varying external forcing or a

state-dependent variability. It must hence be interpreted with great care, as the spectrum does not represent the expected amplitude of fluctuations everywhere in the time series.

## 3.5 Distinguishing Holocene and Late Quaternary climate

In the majority of the Holocene, spectra of proxies show that centennial to millennial-scale fluctuations are within the uncertainties of what can be expected from a single power-law spectrum (Nilsen et al., 2016). In glacial climates on the other hand, Nilsen et al. (2016) and Shao and Ditlevsen (2016) demonstrate that there is a higer scaling exponent from centennial to millennial scales.

To illustrate why, I will use a wavelet analysis, which can give us insight into the fluctuation level as a function of time ($t$) in addition to the time scale ($\Delta t$). I will consider the GRIP ice core data from Greenland, plotted in the upper panel of Figure 3.1. The bottom panel shows the squared magnitude of the continuous wavelet transform

$$W(t, \Delta t) = \frac{1}{\sqrt{\Delta t}} \int_{-\infty}^{\infty} x(t')\psi\left(\frac{t - t'}{\Delta t}\right) dt' \tag{3.2}$$

where $x(t)$ is a signal and $\psi$ is the mother wavelet. It is a small wave package that we slide along the time series, and rescale by the time scale $\Delta t$. I define here $\Delta t$ such that it corresponds to the periods (= 1/frequencies) in the spectrum. By comparing the two panels in Figure 3.1, we observe that the time points with the most power correspond to the abrupt changes in the time series. Even though the changes happen over a short time interval, they increase the power of fluctuations on all scales analyzed.

The white curves in the figure show the limits of what time scales the time series can resolve. The bottom curve is a localized Nyquist frequency = 2·time resolution, increasing as we go back in time because the resolution becomes poorer. Everything below this line has low power due to interpolation of the time series. Methods that only study fluctuations as a function of time scale do not take into account this time variation of the resolution, and get a bias towards lower power on the shortest scales if the time series is interpolated to obtain even sampling. Figure 9 of Nilsen et al. (2016) demonstrates how this may affect the spectrum. Methods designed for analyzing unevenly sampled time series also exist, but these may have other biases (Rehfeld et al., 2011).

One way to overcome this issue is to use the wavelet variance as an estimate for the fluctuation level at each time scale, by averaging the wavelet power over

only the time points where we have good enough resolution to estimate the actual fluctuation level. The two panels of Figure 3.2 show the results for different choices of the mother wavelet. The Mexican hat has good time resolution, but poorer time scale resolution. It is the other way around for the Morlet wavelet.

We can see from both Figure 3.1 and 3.2 that there is little power in the Holocene. The increased power in the ice age is due to dynamics specific for that climate state, because it is associated with abrupt changes in sea ice in North Atlantic – an ice-free area in the Holocene. If removing the abrupt changes, M. Rypdal and K. Rypdal (2016) demonstrate that also ice-age temperatures can be described as a $1/f$ process as in the Holocene. This indicates that as long as we are not close to these tipping points, the dynamics of the ice age may also be described by a linear model. And when approaching a tipping point, we may detect early-warning signals of one or more parameters that are slowly changing before the abrupt change happens (M. Rypdal, 2016).

Although there is a clear distinction between Holocene and ice-age temperatures in this Greenland ice core, it may not be the case everywhere. In the EPICA core from Antarctica for instance, this distinction is less clear. Hence one could ask what time series are the most representative of the two climate states? There may be different problems with each of the proxies, for instance whether they really are good proxies for temperature, or if the proxy contains noise or is smoothed. Furthermore, there is also the possibility that even on the long time scales resolved by the proxies, the fluctuations may differ from one location to another, and are perhaps not well representing global climate.

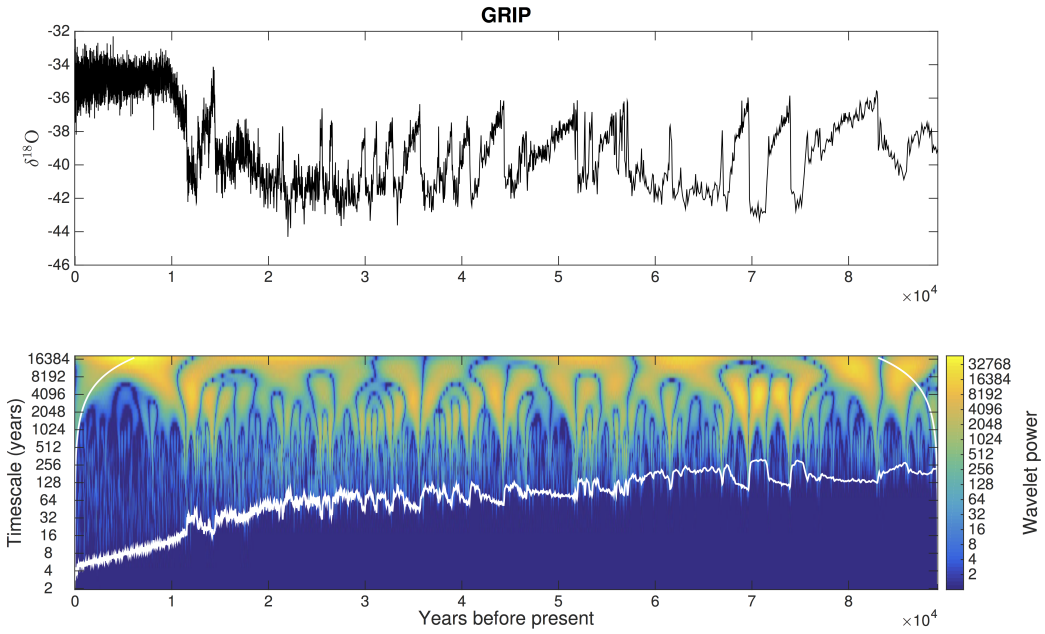


**Figure 3.1:** Upper panel: The $\delta^{18}O$ temperature proxy from the GRIP ice core. Bottom panel: Wavelet power of the time series above computed using the Mexican hat wavelet.

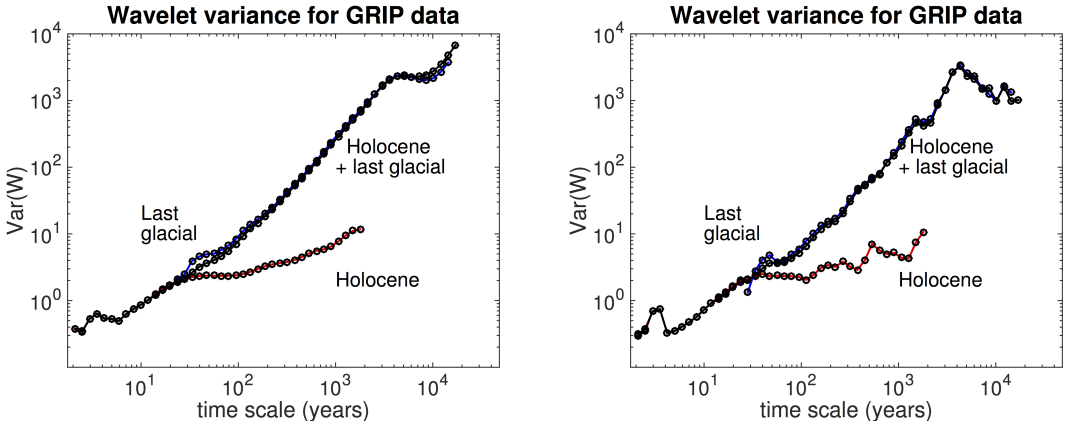


**Figure 3.2:** This figure shows the wavelet variance computed using the wavelet coefficients within the boundaries plotted in Figure 3.1. In the left figure the Mexican hat wavelet is used, while in the right figure the Morlet wavelet is used.

## 3.6 Impacts

For a process with LRD, we have a scaling relation $F(a \cdot \tau) = (a \cdot \tau)^\alpha = a^\alpha \tau^\alpha$. This means that if we rescale $\tau$ by a factor $a$, the fluctuation level will be rescaled by a factor $a^\alpha$. Hence, if we know the fluctuation level at one scale, we can easily predict the level at other scales as well.

One useful application of this is a statistical description of the centennial scale internal variability as predicted from observed variability on shorter scales, which can have an impact on trend-significance studies. In many local temperature records, trends are less significant when testing against a LRD process rather than a simple AR(1) process (Franzke, 2012; Løvsletten and Rypdal, 2016). The reason is that we expect stronger fluctuations on long scales from an LRD process than an AR(1) process. On a global scale however, the global warming trend becomes more apparent as the locally large internal fluctuations are averaged out. Even with a LRD model, Løvsletten and Rypdal (2016) find a highly significant trend with $p$-value $p < 10^{-4}$.

Because the probability of detecting a trend is reduced when using models exhibiting LRD, this hypothesis may seem unnecessary, and in favor of climate change deniers (Mann, 2011). With the low agreement about why we should expect LRD I understand the concern, and we take this as motivation for our studies. Several previous studies can be criticized for applying statistical models uncritically, or just attempting to describe statistical properties without exploring how they are generated. In order to understand how the signal (driven by external forcing) should be distinguished from the noise, the LRD hypothesis should be combined with knowledge about the underlying physics. As noted by Benestad et al. (2016), incautious use of only statistical models may lead to inaccurately treating forced signals as noise, and result in amplified estimates of the noise levels.

The description of LRD as the output from a linear impulse response model with a power-law response provides insight into the expected response to any forcing and future scenarios. In addition, this response model can easily be explained in terms of a simple linear EBM (Fredriksen and Rypdal, 2017). The future consequences of this response to anthropogenic forcing is demonstrated by Rypdal and Rypdal (2014) and K. Rypdal (2016), and show that a long-memory response also leads to long responses to anthropogenic forcing, resulting in a long warming in the pipeline. Compared to simple exponential models that neglect the slowly responding components, a power-law response implies that we must reduce emissions more drastically to reach the goals set in the Paris agreement.

# Chapter 4

# Concluding remarks

In our temperature analyzes we find that most records dominated by internal variability, both instrumental and from climate models, can be well described as scale-invariant. The scaling exponent is increasing with the degree of spatial averaging, and is higher for sea than for land. In the literature studying LRD there are various hypotheses of how this property can arise, resulting in some skepticism of why we need the long-memory models rather than the more commonly used AR(1) processes.

Rypdal (2012) and Rypdal and Rypdal (2014) demonstrated how these statistical processes may arise from an impulse-response model with a power-law response – a useful description both for interpretation of the origin of these processes and their implications for responses to external forcing. In the literature published before one started studying LRD in temperatures, we find various ocean models corresponding to response functions closely resembling what we get from the power-law impulse response model. Hence, we can conclude that a long-memory response is not really something new, the physical models including it have just not been well connected to the concept of LRD in statistical models. The use of fGns and classification of time series as long-range dependent seems initially to be rooted in an interest in the fractal structure of time series, more than in physical principles.

The global power-law response is also well approximated by multibox energy balance models (Fredriksen and Rypdal, 2017). Three time scales are sufficient to approximate infinitely many scales over a range of $2-3$ orders of magnitude, ranging from months to centuries. The stochastic model resulting from this is a sum of three AR(1) processes, not as far away from more widely accepted models after all.

# Bibliography


Andrews, T., J. M. Gregory, and M. J. Webb (2015). The Dependence of Radiative Forcing and Feedback on Evolving Patterns of Surface Temperature Change in Climate Models. *J. Climate*, **28** (4), 1630–1648. doi:10.1175/JCLI-D-14-00545.1.

Andrews, T., J. M. Gregory, M. J. Webb, and K. E. Taylor (2012). Forcing, feedbacks and climate sensitivity in CMIP5 coupled atmosphere-ocean climate models. *Geophys. Res. Lett.*, **39**, L09 712. doi:10.1029/2012GL051607.

Armour, K. C. (2017). Energy budget constraints on climate sensitivity in light of inconstant climate feedbacks. *Nat. Clim. Change*, **7**, 331–335. doi:10.1038/nclimate3278.

Armour, K. C., C. M. Bitz, and G. H. Roe (2013). Time-Varying Climate Sensitivity from Regional Feedbacks. *J. Climate*, **26**, 4518–4534. doi:10.1175/JCLI-D-12-00544.1.

Benestad, R. E., D. Nuccitelli, S. Lewandowsky, K. Hayhoe, H. O. Hygen, R. van Dorland, and J. Cook (2016). Learning from mistakes in climate research. *Theor. Appl. Climatol.*, **126**, 699–703. doi:10.1007/s00704-015-1597-5.

Blender, R. and K. Fraedrich (2003). Long time memory in global warming simulations. *Geophys. Res. Lett.*, **30** (14), 1769. doi:10.1029/2003GL017666.

Bodri, L. (1994). Fractal analysis of climatic data: Mean annual temperature records in Hungary. *Theor. Appl. Climatol.*, **49**, 53–57. doi:10.1007/BF00866288.

Bodri, L. (1995). Short-term climate variability and its stochastic modeling. *Theor. Appl. Climatol.*, **51**, 51–58. doi:10.1007/BF00865539.

Box, G. E. P. (1979). Robustness in the strategy of scientific model building. In *Robustness in Statistics*, editors R. L. Launer and G. N. Wilkinson, Academic Press, pp. 201–236.

Budyko, M. I. (1969). The effect of solar radiation variations on the climate of the Earth. *Tellus*, **21** (5), 611–619. doi:10.1111/j.2153-3490.1969.tb00466.x.

Dickinson, R. E. (1981). Convergence Rate and Stability of Ocean-Atmosphere Coupling Schemes with a Zero-Dimensional Climate Model. *J. Atmos. Sci.*, **38** (10), 2112–2120. doi:10.1175/1520-0469(1981)038<2112:CRASOO>2.0.CO;2.

Dokken, T. M., K. H. Nisancioglu, C. Li, D. S. Battisti, and C. Kissel (2013). Dansgaard-Oeschger cycles: Interactions between ocean and sea ice intrinsic to the Nordic seas. *Paleoceanography*, **28**, 491–502. doi:10.1002/palo.20042.

Eby, M., A. J. Weaver, K. Alexander, K. Zickfeld, A. Abe-Ouchi, A. A. Cimatoribus, E. Crespin, S. S. Drijfhout, N. R. Edwards, A. V. Eliseev, G. Feulner, T. Fichefet, C. E. Forest, H. Goosse, P. B. Holden, F. Joos, M. Kawamiya, D. Kicklighter, H. Kienert, K. Matsumoto, I. I. Mokhov, E. Monier, S. M. Olsen, J. O. P. Pedersen, M. Perrette, G. Philippon-Berthier, A. Ridgwell, A. Schlosser, T. Schneider von Deimling, G. Shaffer, R. S. Smith, R. Spahni, A. P. Sokolov, M. Steinacher, K. Tachiiri, K. Tokos, M. Yoshimori, N. Zeng, and F. Zhao (2013). Historical and idealized climate model experiments: an intercomparison of Earth system models of intermediate complexity. *Clim. Past*, **9**, 1111–1140. doi:10.5194/cp-9-1111-2013.

Fluegeman, R. H. J. and R. S. Snow (1989). Fractal Analysis of Long-Range Paleoclimatic Data: Oxygen Isotope Record of Pacific Core V28-239. *Pure Appl. Geophys.*, **131** (1-2), 307–313. doi:10.1007/978-3-0348-6389-6_17.

Fraedrich, K. and R. Blender (2003). Scaling of Atmosphere and Ocean Temperature Correlations in Observations and Climate Models. *Phys. Rev. Lett.*, **90** (10), 108 501. doi:10.1103/PhysRevLett.90.108501.

Fraedrich, K., U. Luksch, and R. Blender (2004). 1/f model for long-time memory of the ocean surface temperature. *Phys. Rev. E*, **70**, 037 301. doi:10.1103/PhysRevE.70.037301.

Franzke, C. (2012). Nonlinear Trends, Long-Range Dependence, and Climate Noise Properties of Surface Temperature. *J. Climate*, **25**, 4172–4183. doi:10.1175/JCLI-D-11-00293.1.

Fredriksen, H.-B. and K. Rypdal (2016). Spectral characteristics of instrumental and climate model surface temperatures. *J. Climate*, **29**, 1253–1268. doi:10.1175/JCLI-D-15-0457.1.

Fredriksen, H.-B. and M. Rypdal (2017). Long-range persistence in global surface temperatures explained by linear multibox energy balance models. *J. Climate*, **30**, 7157–7168. doi:10.1175/JCLI-D-16-0877.1.

Geoffroy, O., D. Saint-Martin, D. J. L. Olivié, A. Voldoire, G. Bellon, and S. Tytéca (2013). Transient Climate Response in a Two-Layer Energy-Balance Model. Part I: Analytical Solution and Parameter Calibration Using CMIP5 AOGCM Experiments. *J. Climate*, **26**, 1841–1857. doi:10.1175/JCLI-D-12-00195.1.

Good, P., J. M. Gregory, and J. A. Lowe (2011). A step-response simple climate model to reconstruct and interpret AOGCM projections. *Geophys. Res. Lett.*, **38**, L01 703. doi:10.1029/2010GL045208.

Gregory, J. M. (2000). Vertical heat transports in the ocean and their effect on time-dependent climate change. *Clim. Dynam.*, **16**, 501–515. doi:10.1007/s003820000059.

Gregory, J. M. and T. Andrews (2016). Variation in climate sensitivity and feedback parameters during the historical period. *Geophys. Res. Lett.*, **43**, 3911–3920. doi:10.1002/2016GL068406.

Gregory, J. M., W. J. Ingram, M. A. Palmer, G. S. Jones, P. A. Stott, R. B. Thorpe, J. A. Lowe, T. C. Johns, and K. D. Williams (2004). A new method for diagnosing radiative forcing and climate sensitivity. *Geophys. Res. Lett.*, **31**, L03 205. doi:10.1029/2003GL018747.

Gregory, J. M. and J. F. B. Mitchell (1997). The climate response to $CO_2$ of the Hadley Centre coupled AOGCM with and without flux adjustment. *Geophys. Res. Lett.*, **24** (15), 1943–1946. doi:10.1029/97GL01930.

Grieser, J. and C.-D. Schönwiese (2001). Process, Forcing, and Signal Analysis of Global Mean TemperatureVariations by Means of a Three-Box Energy Balance Model. *Clim. Change*, **48**, 617–646. doi:10.1023/A:1005629309829.

Hansen, J., M. Sato, P. Kharecha, and K. von Schuckmann (2011). Earth's energy imbalance and implications. *Atmos. Chem. Phys.*, **11**, 13 421–13 449. doi:10.5194/acp-11-13421-2011.

Hasselmann, K. (1976). Stochastic climate models Part I. Theory. *Tellus*, **28** (6), 473–485. doi:10.1111/j.2153-3490.1976.tb00696.x.

Hasselmann, K., S. Hasselmann, R. Giering, V. Ocana, and H. Von Storch (1997). Sensitivity Study of Optimal CO2 Emission Paths Using a Simplified Structural Integrated Assessment Model (SIAM). *Clim. Change*, **37** (2), 345–386. doi:10.1023/A:1005339625015.

Hasselmann, K., R. Sausen, E. Maier-Reimer, and R. Voss (1993). On the cold start problem in transient simulations with coupled atmosphere-ocean models. *Clim. Dynam.*, **9** (2), 53–61. doi:10.1007/BF00210008.

Held, I. M., M. Winton, K. Takahashi, T. Delworth, F. Zeng, and G. K. Vallis (2010). Probing the Fast and Slow Components of Global Warming by Returning Abruptly to Preindustrial Forcing. *J. Climate*, **23**, 2418–2427. doi:10.1175/2009JCLI3466.1.

Heneghan, C. and G. McDarby (2000). Establishing the relation between detrended fluctuation analysis and power spectral density analysis for stochastic processes. *Phys. Rev. E*, **62** (5), 6103–6110. doi:10.1103/PhysRevE.62.6103.

Hoffert, M. I., A. J. Callegari, and C.-T. Hsieh (1980). The role of deep sea heat storage in the secular response to climatic forcing. *J. Geophys. Res.*, **85** (C11), 6667–6679. doi:10.1029/JC085iC11p06667.

Hooss, G., R. Voss, K. Hasselmann, E. Maier-Reimer, and F. Joos (2001). A nonlinear impulse response model of the coupled carbon cycle-climate system (NICCS). *Clim. Dynam.*, **18** (3-4), 189–202. doi:10.1007/s003820100170.

Hu, K., P. Ivanov, Z. Chen, P. Carpena, and H. E. Stanley (2001). Effect of trends on detrended fluctuation analysis. *Phys. Rev. E*, **64** (1), 011 114. doi:10.1103/PhysRevE.64.011114.

Hurst, H. E. (1951). Long-term storage capacity of reservoirs. *Trans. Amer. Soc. Civil Eng.*, **116**, 770—808.

Hurst, H. E., R. P. Black, and Y. M. Simaika (1965). *Long-term storage*. Constable.

Huybers, P. and W. Curry (2006). Links between annual, Milankovitch and continuum temperature variability. *Nature*, **441**, 329–332. doi:10.1038/nature04745.

IPCC, 2013: Climate change 2013: The physical science basis. Contribution of Working Group I to the Fifth Assessment Report of the Intergovernmental Panel on Climate Change [Stocker, T. F., D. Qin, G.-K. Plattner, M. Tignor, S. K. Allen, J. Boschung, A. Nauels, Y. Xia, V. Bex, and P. M. Midgley (eds.)]. Cambridge University Press, Cambridge, United Kingdom and New York, NY, USA, 1535 pp. doi:10.1017/CBO9781107415324.

Joos, F., R. Roth, J. S. Fuglestvedt, G. P. Peters, I. G. Enting, W. von Bloh, V. Brovkin, E. J. Burke, M. Eby, N. R. Edwards, T. Friedrich, T. L. Fr licher,

P. R. Halloran, P. B. Holden, C. Jones, T. Kleinen, F. T. Mackenzie, K. Matsumoto, M. Meinshausen, G. K. Plattner, A. Reisinger, J. Segschneider, G. Shaffer, M. Steinacher, K. Strassmann, K. Tanaka, A. Timmermann, and A. J. Weaver (2013). Carbon dioxide and climate impulse response functions for the computation of greenhouse gas metrics: a multi-model analysis. *Atmos. Chem. Phys.*, **13**, 2793–2825. doi:10.5194/acp-13-2793-2013.

Kantelhardt, J. W., E. Koscielny-Bunde, H. H. A. Rego, S. Havlin, and A. Bunde (2001). Detecting long-range correlations with detrended fluctuation analysis. *Phys. A*, **295**, 441–454. doi:10.1016/S0378-4371(01)00144-3.

Kim, K. Y. and G. R. North (1991). Surface temperature fluctuations in a stochastic climate model. *J. Geophys. Res.*, **96** (D10), 18 573—18 580. doi:10.1029/91JD01959.

Kim, K. Y. and G. R. North (1992). Seasonal cycle and second-moment statistics of a simple coupled climate system. *J. Geophys. Res.*, **97** (D18), 20 437–20 448. doi:10.1029/92JD02281.

Kim, K. Y., G. R. North, and J. Huang (1992). On the transient response of a simple coupled climate system. *J. Geophys. Res.*, **97** (D9), 10 069–10 081. doi:10.1029/92JD00581.

Koscielny-Bunde, E., A. Bunde, S. Havlin, H. Roman, Y. Goldreich, and H.-J. Schellnhuber (1998). Indication of a Universal Persistence Law Governing Atmospheric Variability. *Phys. Rev. Lett.*, **81** (3), 729–732. doi:10.1103/PhysRevLett.81.729.

Lemke, P. (1977). Stochastic climate models, part 3. Application to zonally averaged energy models. *Tellus*, **29** (5), 385–392. doi:10.1111/j.2153-3490.1977.tb00749.x.

Li, S. and A. Jarvis (2009). Long run surface temperature dynamics of an A-OGCM: the HadCM3 4×CO2 forcing experiment revisited. *Clim. Dynam.*, **33**, 817–825. doi:10.1007/s00382-009-0581-0.

Lovejoy, S. and D. Schertzer (2013). *Low-Frequency Weather and the Emergence of the Climate*, pp. 231–254. American Geophysical Union. ISBN 9781118670187. doi:10.1029/2011GM001087.

Lovejoy, S., D. Schertzer, and D. Varon (2013). Do GCMs predict the climate ... or macroweather? *Earth Syst. Dynam.*, **4**, 439–454. doi:10.5194/esd-4-439-2013.

Løvsletten, O. and M. Rypdal (2016). Statistics of Regional Surface Temperatures after 1900: Long-Range versus Short-Range Dependence and Significance of Warming Trends. *J. Climate*, **29**, 4057–4068. doi:10.1175/JCLI-D-15-0437.1.

Lucarini, V., F. Ragone, and F. Lunkeit (2016). Predicting Climate Change Using Response Theory: Global Averages and Spatial Patterns. *J. Stat. Phys.*, **166**, 1036–1064. doi:10.1007/s10955-016-1506-z.

Malamud, B. D. and D. L. Turcotte (1999). Self-affine time series: I. generation and analyses. *Adv. Geophys.*, **40**, 1–90. doi:10.1016/S0065-2687(08)60293-9.

Mandelbrot, B. B. and J. W. Van Ness (1968). Fractional Brownian Motions, Fractional Noises and Applications. *SIAM Rev.*, **10** (4), 422–437. doi:10.1137/1010093.

Mandelbrot, B. B. and J. R. Wallis (1969). Some long-run properties of geophysical records. *Water Resour. Res.*, **5** (2), 321–340. doi:10.1029/WR005i002p00321.

Mann, M. E. (2011). On long range dependence in global surface temperature series. *Clim. Change*, **107**, 267–276. doi:10.1007/s10584-010-9998-z.

Meehl, G. A., W. M. Washington, C. M. Ammann, J. M. Arblaster, T. M. L. Wigley, and C. Tebaldi (2004). Combinations of Natural and Anthropogenic Forcings in Twentieth-Century Climate. *J. Climate*, **17**, 3721–3727. doi:10.1175/1520-0442(2004)017<3721:CONAAF>2.0.CO;2.

Meinshausen, M., S. C. B. Raper, and T. M. L. Wigley (2011). Emulating coupled atmosphere-ocean and carbon cycle models with a simpler model, MAGICC6 – Part 1: Model description and calibration. *Atmos. Chem. Phys.*, **11**, 1417–1456. doi:10.5194/acp-11-1417-2011.

Monetti, R. A., S. Havlin, and A. Bunde (2003). Long-term persistence in the sea surface temperature fluctuations. *Phys. A*, **320**, 581–589. doi:10.1016/S0378-4371(02)01662-X.

Nilsen, T., K. Rypdal, and H.-B. Fredriksen (2016). Are there multiple scaling regimes in Holocene temperature records? *Earth Syst. Dynam.*, **7**, 419–439. doi:10.5194/esd-7-419-2016.

North, G. R. and R. F. Cahalan (1981). Predictability in a Solvable Stochastic Climate Model. *J. Atmos. Sci*, **38**, 504–513. doi:10.1175/1520-0469(1981)038<0504:PIASSC>2.0.CO;2.

North, G. R., R. F. Cahalan, and J. A. J. Coakley (1981). Energy Balance Climate Models. *Rev. Geophys. Space Phys*, **19** (1), 91–121. doi: 10.1029/RG019i001p00091.

North, G. R., J. Wang, and M. G. Genton (2011). Correlation Models for Temperature Fields. *J. Climate*, **24**, 5850–5862. doi:10.1175/2011JCLI4199.1.

Pelletier, J. and D. Turcotte (1999). Self-affine time series: II. Applications and Models. *Adv. Geophys.*, **40**, 91–166. doi:10.1016/S0065-2687(08)60294-0.

Pelletier, J. D. (1997). Analysis and Modeling of the Natural Variability of Climate. *J. Climate*, **10**, 1331–1342. doi:10.1175/1520-0442(1997)010<1331:AAMOTN> 2.0.CO;2.

Peng, C.-K., S. Buldyrev, S. Havlin, M. Simons, H. Stanley, and A. Goldberger (1994). Mosaic organisation of dna molecules. *Phys. Rev. E*, **49** (2), 1685—1689. doi:10.1103/PhysRevE.49.1685.

Proistosescu, C. and P. J. Huybers (2017). Slow climate mode reconciles historical and model-based estimates of climate sensitivity. *Sci. Adv.*, **3**, e1602 821. doi: 10.1126/sciadv.1602821.

Ragone, F., V. Lucarini, and F. Lunkeit (2015). A new framework for climate sensitivity and prediction: a modelling perspective. *Clim. Dynam.*, **46**, 1459–1471. doi:10.1007/s00382-015-2657-3.

Raper, S. C. B. and U. Cubasch (1996). Emulation of the results from a coupled general circulation model using a simple climate model. *Geophys. Res. Lett.*, **23** (10), 1107–1110. doi:10.1029/96GL01065.

Raper, S. C. B., J. M. Gregory, and T. J. Osborn (2001). Use of an upwelling-diffusion energy balance climate model to simulate and diagnose A/OGCM results. *Clim. Dynam.*, **17**, 601–613. doi:10.1007/PL00007931.

Raper, S. C. B., J. M. Gregory, and R. J. Stouffer (2002). The Role of Climate Sensitivity and Ocean Heat Uptake on AOGCM Transient Temperature Response. *J. Climate*, **15**, 124–130. doi:10.1175/1520-0442(2002)015<0124: TROCSA>2.0.CO;2.

Rehfeld, K., N. Marwan, J. Heitzig, and J. Kurths (2011). Comparison of correlation analysis techniques for irregularly sampled time series. *Nonlinear Process. Geophys.*, **18**, 389–404. doi:10.5194/npg-18-389-2011.

Richardson, M., K. Cowtan, E. Hawkins, and M. B. Stolpe (2016). Reconciled climate response estimates from climate models and the energy budget of Earth. *Nat. Clim. Change*, **6**, 931–935. doi:10.1038/nclimate3066.

Rybski, D., A. Bunde, and H. von Storch (2008). Long-term memory in 1000-year simulated temperature records. *J. Geophys. Res.*, **113**, D02 106. doi:10.1029/2007JD008568.

Rypdal, K. (2012). Global temperature response to radiative forcing: Solar cycle versus volcanic eruptions. *J. Geophys. Res.*, **117**, D06 115. doi:10.1029/2011JD017283.

Rypdal, K. (2015). Attribution in the presence of a long-memory climate response. *Earth Syst. Dynam.*, **6**, 719–730. doi:10.5194/esd-6-719-2015.

Rypdal, K. (2016). Global warming projections derived from an observation-based minimal model. *Earth Syst. Dynam.*, **7**, 51–70. doi:10.5194/esd-7-51-2016.

Rypdal, K. and M. Rypdal (2016). Comment on "Scaling regimes and linear/nonlinear responses of last millennium climate to volcanic and solar forcing" by S. Lovejoy and C. Varotsos (2016). *Earth Syst. Dynam.*, **7**, 597–609. doi:10.5194/esd-7-597-2016.

Rypdal, K., M. Rypdal, and H.-B. Fredriksen (2015). Spatiotemporal Long-Range Persistence in Earth's Temperature Field: Analysis of Stochastic–Diffusive Energy Balance Models. *J. Climate*, **28**, 8379–8395. doi:10.1175/JCLI-D-15-0183.1.

Rypdal, M. (2016). Early-Warning Signals for the Onsets of Greenland Interstadials and the Younger Dryas–Preboreal Transition. *J. Climate*, **29**, 4047–4056. doi:10.1175/JCLI-D-15-0828.1.

Rypdal, M. and K. Rypdal (2014). Long-Memory Effects in Linear Response Models of Earth's Temperature and Implications for Future Global Warming. *J. Climate*, **27**, 5240–5258. doi:10.1175/JCLI-D-13-00296.1.

Rypdal, M. and K. Rypdal (2016). Late Quaternary temperature variability described as abrupt transitions on a 1/f noise background. *Earth Syst. Dynam.*, **7**, 281–293. doi:10.5194/esd-7-281-2016.

Sellers, W. D. (1969). A Global Climatic Model Based on the Energy Balance of the Earth-Atmosphere System. *J. Appl. Meteorol.*, **8**, 392–400. doi:10.1175/1520-0450(1969)008<0392:AGCMBO>2.0.CO;2.

Shao, Z.-G. and P. D. Ditlevsen (2016). Contrasting scaling properties of interglacial and glacial climates. *Nat. Commun.*, **7**, 10 951. doi:10.1038/ncomms10951.

Stocker, T. F. and S. J. Johnsen (2003). A minimum thermodynamic model for the bipolar seesaw. *Paleoceanography*, **18** (4), 1087. doi:10.1029/2003PA000920.

Torrence, C. and G. P. Compo (1998). A Practical Guide to Wavelet Analysis. *Bull. Am. Meteorol. Soc.*, **79** (1), 61–78. doi:10.1175/1520-0477(1998)079<0061:APGTWA>2.0.CO;2.

van Vliet, K. M., A. van der Ziel, and R. R. Schmidt (1980). Temperature-fluctuation noise of thin films supported by a substrate. *J. Appl. Phys.*, **51** (6), 2947–2956. doi:10.1063/1.328104.

Vyushin, D. I., P. J. Kushner, and J. Mayer (2009). On the origins of temporal power-law behavior in the global atmospheric circulation. *Geophys. Res. Lett.*, **36**, L14 706. doi:10.1029/2009GL038771.

Vyushin, D. I., P. J. Kushner, and F. Zwiers (2012). Modeling and understanding persistence of climate variability. *J. Geophys. Res.*, **117**, D21 106. doi:10.1029/2012JD018240.